

Chaos and Non-linear Dynamics of a 1.55 μm InGaAsP-InP Microring Laser

Konstantinos E. Chlouverakis^{*a}, Spiros Mikroulis^a and Dimitris Syvridis^a

^aDepartment of Informatics and Telecommunications, University of Athens, Illisia, 15784, Athens, Greece

ABSTRACT

In this paper, numerical investigation is performed for a 1.55 μm InGaAsP-InP microring laser as a function of the bus waveguide reflectivity, the injection current and the phase of the backreflected field. The nascent nonlinear instabilities are identified utilizing a multimode rate equation model, originating from the continuous injections of each clockwise to the counterclockwise mode and inverse. The resulted time series are filtered using a 40GHz electrical low pass filter in order to omit the mode beatings. Chaos data analysis revealed high-dimensional chaos by means of the correlation dimension and the metric entropy calculation with continuously testing surrogate data. With increasing the bus waveguide reflectivity, period-doubling and quasiperiodic route to chaos was found and the dimension was found to follow a linear increase. The same dimension increase was found with increasing the injection current, with the system experiencing sudden transitions from chaos to limit cycles. With altering the phase of the backreflected field the dynamics were found to transit from limit cycle ($\Delta\phi=0\rightarrow\pi/2$) to chaos, maintained chaotic ($\Delta\phi=\pi/2\rightarrow2\pi/3$) and finally returning to periodic states ($\Delta\phi=2\pi/3\rightarrow2\pi$). Furthermore, the dynamics are investigated with calculating the standardized moments.

Keywords: microring lasers, correlation dimension, torus, chaos data analysis, chaos

1. INTRODUCTION

Semiconductor microring lasers (SMLs) are promising candidates for optoelectronic integrated circuits since they combine small footprint, high spectral purity occurring from the traveling wave nature of the device, and simple fabrication due to the absence of cleaved-facets and gratings. A wide range of microring-based lightwave system applications can be performed, such as low-cost modulation sources for short to medium optical links, all-optical switches and optical memories¹. Apart from the technological evaluation of the device, in a general point of view, a microring laser can be considered as a complicated physical system with a high level degree of freedom resulting from the multi-longitudinal mode dynamics²⁻⁴, combined with the nonlinear mode interaction and backreflection through bus waveguide facets.

Nowadays, there is significant interest in developing optical chaotic generators because of their potential applications as carriers in secure communication schemes and also for the construction of optical gates⁵, revealing the importance of nonlinear dynamics in high-speed optical communications. On the other hand, the current trend in photonics technology is towards integrated photonic devices and such a chaotic integrated optical generator was recently realized experimentally using a colliding-pulse mode-locked semiconductor laser⁶.

In this paper, we investigate the chaotic dynamics and especially the route to chaos of a 1.55 μm InGaAsP-InP SML via the break-up of a 2-torus with increasing the bus waveguide's residual reflectivity R . This specific route to chaos has been also numerically demonstrated for optically-injected semiconductor lasers⁷ and lasers subjected to filtered feedback⁸. The investigation will take place with phase diagrams, calculation of the largest Lyapunov exponent and the correlation dimension. Lastly, the dimensionless standardized moments of skewness and kurtosis⁹ will be calculated and interconnected with the torus breakup for the best time to the best of our knowledge.

[*chlouver@di.uoa.gr](mailto:chlouver@di.uoa.gr); phone +30 210 7275322

2. NUMERICAL MODEL

The investigation of the dynamics herein is continued as a function of the bus waveguide reflectivity R , the injection current I and the phase of the backreflected field φ , and the nascent nonlinear instabilities are identified utilizing the multimode rate equation model^{2,3} given below, where p is the mode number and m corresponds to each propagation direction, either clockwise (CW) or counterclockwise (CCW):

$$\begin{aligned} \frac{dE_{p,\pm m}}{dt} &= \frac{1}{2}(1+i\alpha) \left[G_{p,\pm m} - \frac{1}{\tau_p} \right] E_{p,\pm m} + \frac{K^{\mp m}}{\tau_p} E_{p,\pm m}(t-\tau_d) e^{-i\omega_p \tau_d} + F_p(t) \\ \frac{dN}{dt} &= \frac{I}{eV} - \frac{N}{\tau_s} - \sum G_{p,\pm m} |E_{p,\pm m}|^2 \\ G_{p,\pm m} &= A_p - sg(N-N_0) |E_{p,\pm m}|^2 - \sum_{p,q,\pm m} D_{p(q)} |E_{p,\pm m}|^2 - \sum_{p \neq q, \pm m} H_{p(q)} |E_{p,\pm m}|^2 \end{aligned} \quad (1)$$

Where G is the modal gain variable including the linear $A(\cdot)$, the nonlinear s , the symmetric $D(\cdot)$ and asymmetric $H(\cdot)$ gain suppression coefficients respectively, described in detail^{2,3}, E is the complex electric field amplitude, N the carrier concentration, τ_p and τ_s the photon and electron lifetimes respectively, τ_d the feedback delay time for each mode to be coupled back to the ring, N_0 the carrier concentration at transparency and g the differential gain. The parameter K refers to the linear coupling that includes the bus waveguide's residual reflectivity, R , defined as the ratio of the backreflected to the transmitted power to the bus waveguide facet, acting also as an internal additional optical feedback mechanism to the microring cavity (Fig. 1), and ω_p is the free-running frequency for each mode p where $\omega_p \tau_d$ refers to the phase of each mode. The nonlinear system of equations is solved for equal number of modes propagating in each direction (CW/CCW). The number of supported modes is determined by the gain bandwidth, and the ring's free spectral range $\text{FSR} = \lambda_0^2 / \pi n L$. The ring radius is taken as $r = 50 \mu\text{m}$, the injection current $I = 2.3 I_{\text{TH}}$, where I_{TH} is the threshold current and the bus waveguide length $L_b = 4r$. In the text herein the CCW direction is arbitrarily chosen since the time traces are dynamically identical for both directions (CW/CCW), due to the equal and relatively high values of residual reflectivity ($R = R_{\text{CW}} = R_{\text{CCW}}$) used for both bus waveguide facets². In order to examine the time series, the complex fields of each mode are summed and the total power is calculated through the squared absolute value of the resulted summation.

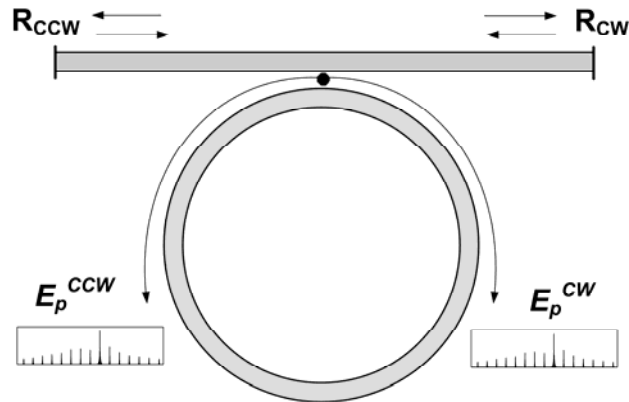


Fig.1 A semiconductor microring laser (schematic)

3. QUASIPERIODIC ROUTE TO CHAOS

The torus doubling route to chaos is a higher-dimensional phenomenon, requiring at least a four-dimensional flow, or a three-dimensional map. In our high-dimensional model, that consists of 60 coupled delay differential equations and one coupled ordinary differential equation (the equation for carriers dN/dt), it is prudent to conclude that the break-up of a 2-

torus should be a common mechanism. For the optically-injected semiconductor laser⁷ the break-up of a torus is demonstrated despite the fact that the system is modelled by a three-dimensional flow. The latter results in a break-up of a torus that is not folded though into a double one before it transits to chaos.

In Fig.2 with increasing R , the system transits from limit cycle, to a torus and suddenly the torus breaks-up into a low-dimensional chaotic attractor with calculated correlation dimension $D_2=3.2\pm 0.2$ and largest Lyapunov exponent $\lambda_1\approx 0.01\text{ps}^{-1}$. These four attractors are reconstructed from a 120ns time-series resulting 2.4×10^5 closely-spaced points. It is plausible to conclude that the latter assures an adequate reconstruction of the attractor together with an accurate estimation of the correlation dimension in the order $D_2\sim 5$ since the calculation for $D_2>6$ is substantially hampered due to significant statistical errors. Correlation time τ is computed when the autocorrelation function¹⁰ reaches the value of e^{-1} . Generally, the correlation dimension D_2 for N points is calculated from the correlation integral-sum $C(r)$, which is the probability that two randomly chosen points on the attractor are separated by a distance less than r and generally is given by:

$$D_2 = \lim_{r \rightarrow 0} \frac{d \log C(r)}{d \log r} \quad (2a)$$

The correlation sum $C_m(r)$ is given for any embedding dimension m by:

$$C_m(r) = \frac{2}{N(N-1)} \sum_{j=1}^N \sum_{i=j+1}^N \Theta(r - r_{ij}) \quad (2b)$$

where $\Theta[...]$ is Heaviside function.

In Fig.3 the cross-section plots, for the condition $dP(t)/dt=0$, are depicted for $R=0.12$ (torus) and $R=0.1295$ (break-up of torus) and in Fig.4 the time-series for the same values of R as in Fig.3.

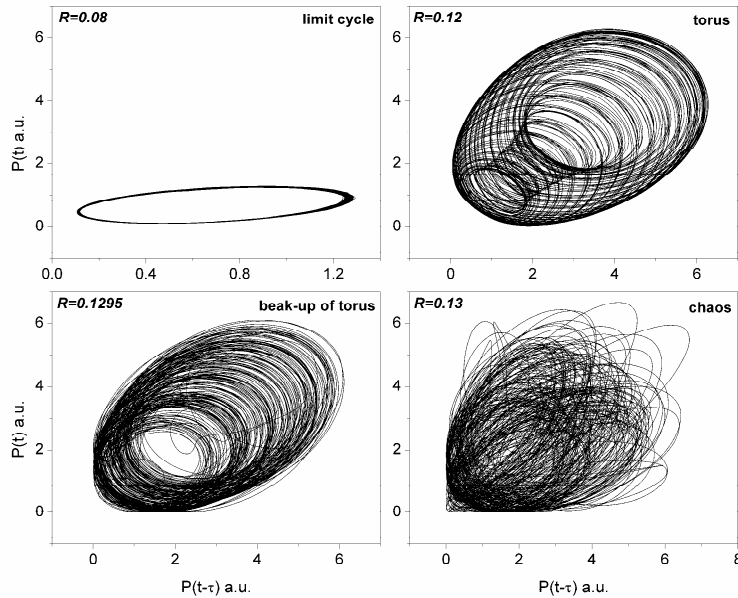


Fig.2 Phase portraits of the SML dynamics as R varies showing the transition from limit cycle, torus, torus annihilation and finally chaos.

For the $R=0.12$ case where the system experiences a 2-torus, two dominant frequencies were found and the correlation matrix showed two dominant components. Other evidence for the torus existence is the value of the attractor dimension equal to $D_2=2.0\pm 0.005$ for all embeddings $m_e>1$, the largest Lyapunov exponent equal to $\lambda_1= (0\pm 0.001) \text{ps}^{-1}$ and that the

correlation function was found to decay very slowly. It is interesting to note that the $R=0.1295$ case closely resembles visually intermittent behaviour, but the erratic periodic bursts that should appear for the latter, do not occur for more than one time-segments, only around $t=80\text{ns}$, possibly justified by the considerable stochastic noise sources or the electric filtering. Nevertheless, the origin of such a transition may be attributed to the existence of a tongue of quasiperiodic motion near a torus-doubling bifurcation line, similarly to the ring map and the Toda oscillator found in the edge of chaos¹¹.

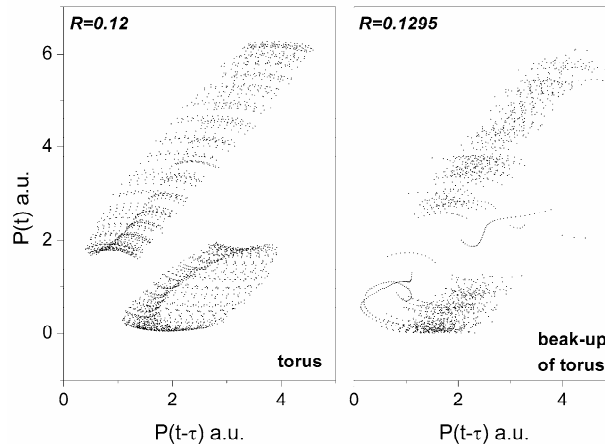


Fig.3 Cross-section plots for the torus ($R=0.12$) and the torus break-up ($R=0.1295$)

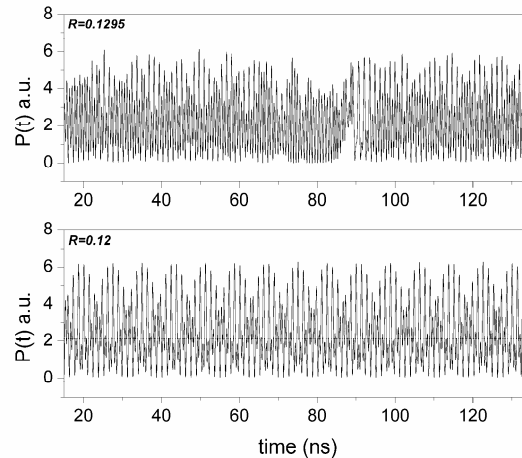


Fig.4 Time series for the torus ($R=0.12$) and the torus break-up ($R=0.1295$)

4. STANDARDIZED MOMENTS

In order to examine in more detail the dynamics of the SML, and especially the transit from torus to chaos from a different dynamics view, the standardized moments are calculated as R increases. These moments⁸ include the excess kurtosis K , which is the degree of peakedness of a distribution, and the skewness S that is a measure of the degree of lopsidedness of the distribution of an attractor of N points, where σ denotes the standard deviation:

$$K = \frac{1}{N} \sum_{i=1}^N \left(\frac{P(i) - \langle P(t) \rangle}{\sigma} \right)^4 - 3 \quad (3a)$$

$$S = \frac{1}{N} \sum_{i=1}^N \left(\frac{P(i) - \langle P(t) \rangle}{\sigma} \right)^3 \quad (3b)$$

The “minus 3” term in Eq. (3a) is explained as a correction to make the kurtosis of the normal distribution equal to zero. Scope of the remainder of this Letter is to demonstrate the topological changes in the attractor that affect the moments above of the probability distribution for the whole transition from limit cycle, to torus, to torus’ collapse and finally to chaos transition. In Fig.5 the skewness and kurtosis are plotted for increasing R . Three local extrema are shown indicating sudden crises on the geometrical topology of the attractor. The first crisis is relevant to the torus birth from a limit cycle, the second one to the torus annihilation (with an additional slight local extreme due to the erratic burst of Fig.4) and the third one to the nascent chaotic dynamics indicating slightly platykurtic distributions. Similarly, for the optically-injected semiconductor laser⁷, these three crises were also calculated in our simulations exhibiting identical qualitative behavior.

Besides the interconnection of the quasiperiodic route to chaos with the dimensionless moments of S and K , it is interesting to investigate the connection of S and K as it was realized for drift-interchange turbulence in TORPEX plasmas¹². In the latter, a relation in the form $K = \alpha S^2 + \beta$ was demonstrated following a special Beta distribution resulting in both positive and negatives values for S . For the microring laser and specifically for the route to chaos via the torus break-up (as also for the injected laser), only positive values of S were exhibited. Albeit it is prudent to conjecture such a relation for the microring laser, this perquisition is patently arduous in terms of numerical computation for hundreds time-series in order to maintain an adequate statistical error. The data are depicted in Fig. 6 and are least-square fitted by the quadratic polynomial for 500 cases:

$$K = (1.32 \pm 0.05)S^2 + (2 \pm 0.045) \quad (4)$$

where K is the kurtosis without the “minus 3” term though in Eq.(3a) in order to coincide with the notation of the probability distributions¹³. It is noted that the data of Fig.6 could follow a variant of the Gamma distribution since skewness is always non-negative. For the Gamma, and also the Chi-square distribution that is a special case of the former, the relation between S and K is trivial in contrast to the Beta distribution¹² and equal to $K = 1.5S^2 + 3$. Hence, the data of Fig.6 may be fitted better with a special Beta distribution, as well, with only positive values of S though. The former requires¹² $1 < \alpha < 1.5$ and $1 < \beta < 3$ for the general relation $K = \alpha S^2 + \beta$. These inequalities fulfill our fitting of Eq.(4) and therefore it is prudent to present our results as a bridge between a special Beta and the Gamma distribution as an upper limit.

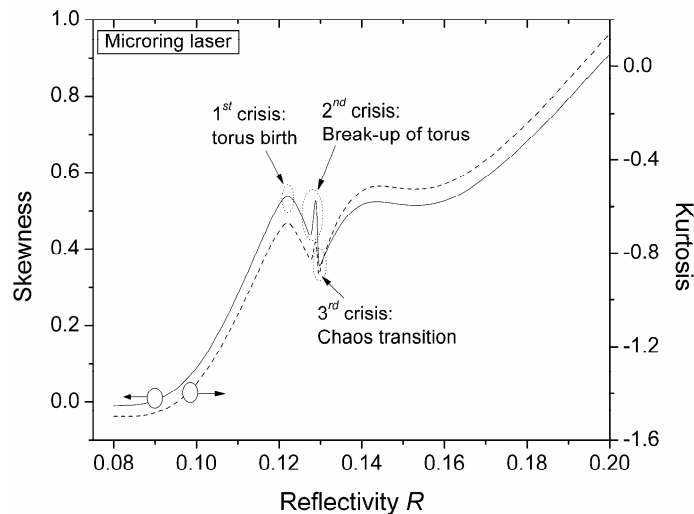


Fig.5 Skewness and kurtosis as R varies for the SML. The three sudden crises are marked with the dotted circles.

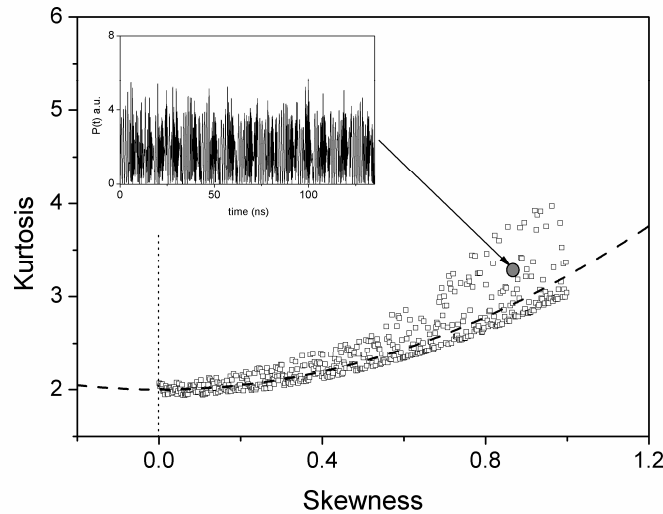


Fig.6 Kurtosis versus skewness computed for 500 cases. The 2nd order fitted polynomial is also depicted together with the inset of a highly leptokurtic and lopsided chaotic attractor.

Another parameter that is important in laser dynamics is the phase ϕ of the backreflected field amplitude. In the case for the attractor of Fig.7a, the dynamics oscillate periodically with $D_2 \approx 1.1$ whereas with altering the phase of the backreflected field (experimentally with a thermally tuned phase shifter) with variation $\Delta\phi = \pi/2$ the attractor becomes chaotic (Fig.7b). By further varying the phase at $\Delta\phi = 2\pi/3$ (Fig.7c) the system preserves its chaotic behaviour whereas finally for $\Delta\phi = \pi$ (Fig.7d) returns to a limit cycle again. It is calculated that for higher lengths of the bus waveguide ($L_b \geq 5r$ for the same intrinsic parameters used herein) this phase dependence deteriorates similarly to lasers subjected to optical feedback from a short external cavity¹⁴, a major characteristic of systems with feedback processes.

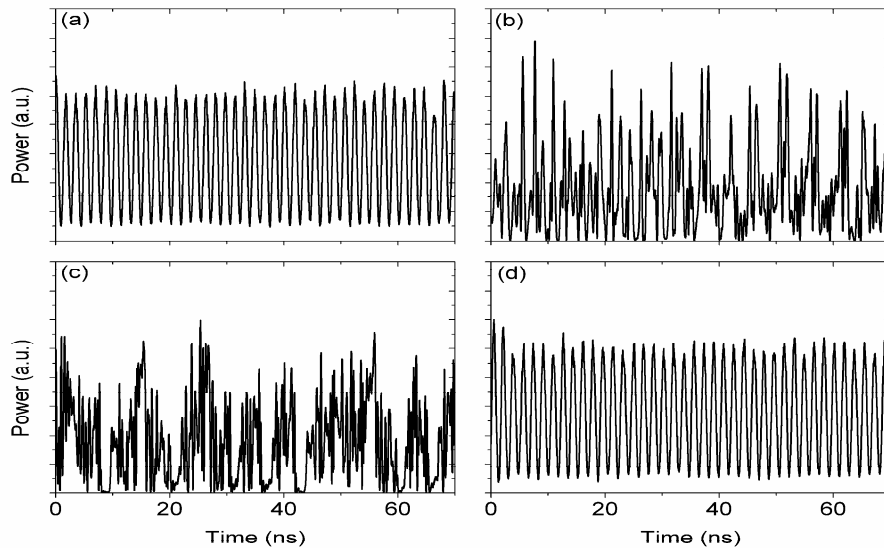


Fig 7. Phase dependence: Time traces for $R=-22\text{dB}$ and $I=2.3I_{TH}$ for a) $\Delta\phi=0$, b) $\Delta\phi=\pi/2$, c) $\Delta\phi=2\pi/3$ and d) $\Delta\phi=\pi$.

For the high dimensional case of $R=-14\text{dB}$ the time evolution of the power for each of the dominant laser modes is plotted in Fig.8a whereas in Fig.8b the chaotic optical spectrum is depicted showing the 15 modes that are considered for

the CCW direction in our model. It is easily noticed that albeit modes 0, +1 and -2 are in some sense correlated, the chaotic output is resulted by their competition and especially from the mode +2 that is dominant. The elaboration of each mode individually results in separate chaotic carriers with comparable dimensions ($D_2 \sim 6$) except for the dominant mode that exhibits $D_2 > 7$.

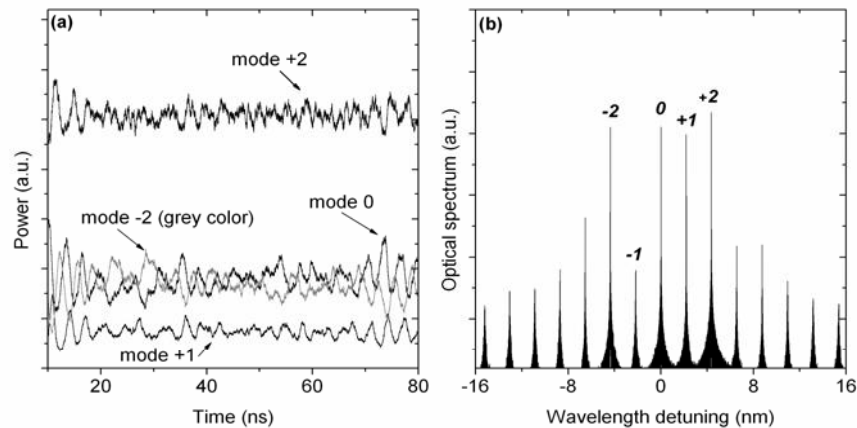


Fig 8 a) Power of the first 4 modes for $R=-14\text{dB}$ and $I=2.3I_{TH}$ (high-dimensional chaos). The -1 mode is not depicted due to its low power, and b) optical spectrum showing the 15 modes with the 5 first of them numbered.

5. CONCLUSIONS

In this Letter the break-up of a torus was demonstrated for a semiconductor microring laser and the quasiperiodic route to chaos was investigated with also calculating the skewness and kurtosis. With repeating these calculations for other chaotic systems, it is concluded that this route to chaos results in three sudden crises in the topology of the attractor. Finally, the link between skewness S and kurtosis K was presented with a quadratic polynomial fitting $K=\alpha S^2+\beta$, indicating an underlying structure of a Beta distribution variant. The results herein might prove beneficial to experimentalists since the skewness and kurtosis can be easily calculated for any given time-series, albeit the primary scope of this Letter was to demonstrate the break-up of a torus in a semiconductor microring laser as the basic route to chaos, and the beginning of understanding further the dynamics^{15,16} of this optical system with a fervent expectation for future applications to chaotic optical communications¹⁷.

REFERENCES

- [1] M. T. Hill, H. J. S. Dorren, T. Vries, X. J. M. Leijtens, J. H. den Besten, B. Smalbrugge, Y.-S. Oei, H. Binsma, G.-D. Khoe and M. K. Smit, "A fast low-power optical memory based on coupled micro-ring lasers," *Nature* 432, 206-209 (2004).
- [2] I. Stamataki, S. Mikroulis, A. Kapsalis, D. Syvridis, "Investigation on the multimode dynamics of InGaAsP/InP microring lasers," *IEEE J. Quantum Electron.* 42, 1266-1273 (2006).
- [3] S. Mikroulis, I. Stamataki, D. Alexandropoulos, M. Hamacher, E. Roditi, D. Syvridis, "Low frequency relative intensity noise due to nonlinear mode competition in InGaAsP/InP microring lasers," *IEEE Photon. Technol. Lett.* 18, 1895-1897 (2006).
- [4] K. E. Chlouverakis, S. Mikroulis, I. Stamataki and D. Syvridis, "Chaotic dynamics of semiconductor microring lasers," *Opt. Lett.* 32, 2912-2914 (2007).
- [5] S. Sinha and W. L. Ditto, "Dynamics based computation," *Phys. Rev. Lett.* 81, 2156-2159 (1998).
- [6] M. Yousefi, Y. Barbarin, S. Beri, E. Bente, M. Smit, R. Notzel and D. Lenstra, "New role for nonlinear dynamics and chaos in integrated semiconductor laser technology," *Phys. Rev. Lett.* 98, 044101 (2007).
- [7] S. Wieczorek, B. Krauskopf and D. Lenstra, "Sudden chaotic transitions in an optically injected semiconductor laser," *Opt. Lett.* 26, 816-818 (2001).
- [8] K. Green, B. Krauskopf and K. Engelborghs, "Bistability and torus break-up in a semiconductor laser with phase-conjugate feedback," *Physica D* 173, 114-129 (2002).
- [9] J. C. Sprott, *Chaos and Time-series Analysis* (Oxford University Press, 2003).
- [10] J.-P. Eckmann and D. Ruelle, "Ergodic theory of chaos and strange attractors," *Rev. Mod. Phys.* 57, 617-656 (1985).
- [11] S.-Y. Kim and W. Lim, "Universal mechanism for the intermittent route to strange nonchaotic attractors in quasiperiodically forced systems," *J. Phys. A* 37 6477-6489 (2004).
- [12] B. Labit, I. Furno, A. Fasoli, A. Diallo, S. H. Müller, G. Plyushchev, M. Podestà and F. M. Poli, "Universal statistical properties of drift-interchange turbulence in TORPEX plasmas," *Phys. Rev. Lett.* 98, 255002 (2007).
- [13] N. L. Johnson, S. Kotz, and N. Balakrishnan, *Continuous Univariate Distributions* (John Wiley & Sons, New York, 1995), 2nd ed.

- [14] R. Vicente, J. Dauden, P. Colet and R. Toral, "Analysis and characterization of the hyperchaos generated by a semiconductor laser subject to a delayed feedback loop," *IEEE J. Quantum. Electr.* 41, 541-548 (2005).
- [15] G. Yuan and S. Yu, "Analysis of Dynamic Switching Behavior of Bistable Semiconductor Ring Lasers Triggered by Resonant Optical Pulse Injection," *IEEE J. Select. Topics Quantum. Electron.* 13, 1227-1234 (2007).
- [16] T. Pérez, A. Scirè, G. Van der Sande, P. Colet, and C. R. Mirasso, "Bistability and all-optical switching in semiconductor ring lasers," *Opt. Express* 15, 12941-12948 (2007).
- [17] A. Argyris, D. Syvridis, L. Larger, V. Annovazzi-Lodi, P. Colet, I. Fischer, J. Garcia-Ojalvo, C. Mirasso, L. Pesquera and K. A. Shore, "Chaos-based communications at high bit rates using commercial fibre-optic links," *Nature* 438, 343-346 (2005).